IRAS F10214+4724: the inner 100 pc

Mon. Not. R. Astron. Soc. **299,** 1220–1230 (1998)

IRAS F10214+4724: the inner 100 pc

Mark Lacy,[1] Steve Rawlings[1] and Stephen Serjeant[2]
[1]*Astrophysics, Department of Physics, Keble Road, Oxford, OX1 3RH*
[2]*Astrophysics Group, Imperial College London, Blackett Laboratory, Prince Consort Road, London SW7 2BZ*

Accepted 1998 June 1. Received 1998 May 11; in original form 1998 March 4

ABSTRACT

We use new high-resolution near-infrared spectroscopy and our previously published optical spectroscopy of the gravitationally lensed Seyfert 2 galaxy F10214+4724 to study both the links between the starburst and AGN in this object and the properties of the line-emitting clouds in the inner narrow-line region. Close inspection of the rest frame UV spectrum reveals interstellar or stellar absorption features consistent with a compact, moderately reddened starburst providing about half the UV light, and explaining the dilution of the UV continuum polarization relative to the broad emission lines. Spectroscopy of the Hα/[N II] line blend has enabled us to assess the relative contributions of the emission from the narrow-line region of the Seyfert 2, and a moderately reddened emission-line region which we argue is associated with the starburst activity. Estimates of the star formation rate from the unpolarized UV continuum flux and the Hα flux are consistent to within their associated uncertainties. We find we can plausibly explain the unusual emission-line properties of F10214+4724 in terms of conventional models for nearby Seyfert 2 galaxies if lensing is preferentially magnifying the side of the inner narrow-line region between the AGN and the observer, and the other side is both less magnified and partially obscured by the torus. The hydrogen densities of clouds in this region are high enough to make the Balmer lines optically thick and to suppress forbidden emission lines with low critical densities. From the emission-line spectrum we have deduced the column density of both ionized and neutral gas in the narrow-line clouds, and the density of the ionized gas. Using these we have been able to estimate the mass of the inner narrow-line clouds to be $\sim 1\,\mathrm{M}_{\odot}$, and show that the gas:dust ratio $N_{\mathrm{H}}/E(B-V)$ in these clouds must be $\sim 1.3\times 10^{27}\,\mathrm{m}^{-2}\,\mathrm{mag}^{-1}$, significantly higher than the average value in the Milky Way, $\sim 4.5\times 10^{25}\,\mathrm{m}^{-2}\,\mathrm{mag}^{-1}$. The column density and low dust content of a typical cloud are consistent with the properties of the warm absorbers seen in the X-ray spectra of Seyfert 1 galaxies. Our results thus favour models in which the narrow-line clouds start life close to the nucleus and flow out. An emission line from the lensing system has allowed us to confirm its redshift as $z \approx 0.9$.

Key words: galaxies: active – galaxies: individual: FSC 10214+4724 – galaxies: Seyfert – galaxies: starburst – gravitational lensing – infrared: galaxies.

1 INTRODUCTION

The gravitationally lensed Seyfert 2 galaxy FSC 10214+4724 has been the subject of extensive study in all accessible wavebands since its discovery (Rowan-Robinson et al. 1991). Initially thought to be the most luminous galaxy in the Universe, it became increasingly clear that gravitational lensing was at least partly responsible for its ultra-high luminosity (Matthews et al. 1994; Trentham 1995; Serjeant et al. 1995, hereafter Paper I; Broadhurst & Lehár 1995; Graham & Liu 1995; Eisenhardt et al. 1996). In parallel with this, the debate continued about the relative contributions of the Seyfert 2 and starburst components to the spectral energy distribution, a debate which is still ongoing (e.g. Rowan-Robinson et al. 1993; Elston et al. 1994; Lawrence et al. 1994; Soifer et al. 1995; Goodrich et al. 1996; Kroker et al. 1996; Green & Rowan-Robinson 1996; Serjeant et al. 1998, hereafter Paper II).

This latter controversy has assumed particular importance recently with the inference of an apparent peak in the star formation rate of the Universe at $z \sim 2$ deduced from the UV fluxes of high-redshift galaxies (Madau, Pozzetti & Dickinson 1998). Based on this, we might expect all massive galaxies at $z \sim 2$ to be associated with star formation rates about 10 times greater than in the local Universe (i.e. a few solar masses per year for a $\sim L_*$ galaxy), consistent with the value obtained from the narrow Hα emission in F10214+4724

(Serjeant et al. 1998). We do not, however, necessarily expect to find the extremely high star formation rates that are implied by the far-infrared luminosity of F10214+4724 if a large fraction of the luminosity is the result of a starburst. Nevertheless, the possibility that a large amount of star formation in the high-redshift Universe is hidden by dust (and therefore missed from UV-based estimates) is suggested by the discovery of an infrared background (Guiderdoni et al. 1997) and by the results of infrared and submm surveys (Rowan-Robinson et al. 1997; Smail, Ivison & Blain 1997). The nuclear regions of AGN with their dense, dusty neutral tori wrapping the central object may turn out to be ideal sites for hiding substantial starbursts.

The gravitational lensing of F10214+4724 also offers us an opportunity to examine the inner regions of a luminous narrow-line AGN at high effective spatial resolution. The arc of F10214+4724 is believed to consist of three merged images within a total arc length of 0.7 arcsec. The total magnification of the arc is $\approx$100, and because the lensing is modelled well by an isothermal potential (Eisenhardt et al. 1996), the magnification of each image occurs predominantly along the direction of the arc, with little magnification or demagnification perpendicular to it. So if F10214+4724 were not magnified, the nuclear region would have an angular size of only $\sim$7 mas, corresponding to a physical size of 50 pc for $H_0 = 50$ km s^{-1} Mpc^{-1} and $q_0 = 0.5$ (assumed throughout this paper). Resolution of AGN on this physical scale is otherwise only possible for the nearest objects, using the *Hubble Space Telescope* (*HST*).

In Paper II we showed that the Lyα photons from F10214+4724 emerge from a neutral column of $\approx 2.5 \times 10^{25}$ m^{-2}, and that the 1:1 doublet ratio of O VI could be produced by absorption in the damping wings of Lyβ as the emission lines propagated through this column. We further argued that the neutral column was probably within the narrow-line region itself, located at the back of radiation-bounded narrow-line clouds. We also presented the results of photoionization modelling which pointed to the narrow-line emission arising in relatively dense, high-ionization narrow-line clouds. Our models (and those of Soifer et al. 1995) were, however, unsuccessful in fully accounting for the weak Balmer line emission and the lack of [O II] 372.7 in the spectrum.

To attempt to resolve some of the remaining questions about F 10214+4724, we obtained near-infrared spectra in the *J*,*H* and *K* bands with the CGS4 spectrometer on the United Kingdom Infrared Telescope (UKIRT). The probable discovery of an emission line from the lensing system is discussed in Section 3. In Section 4 we discuss the Balmer lines, and describe how the spectra were used to estimate the relative contributions of the narrower component of Hα, associated with star formation in Paper II and the Hα from the highly-magnified inner narrow-line region (INLR). We also discuss the related problem of the anomalously low Hβ flux measured by us in Paper II and by others, and place a firm limit on the contribution of any broader component to the Hα flux from the broad-line region of the hidden quasar. Section 5 discusses the other near-infrared lines, and Section 6 the reddening towards the narrow-line region. In Section 7, features in the rest frame UV spectrum of F10214+4724 are discussed and amount of the star-formation activity in F 10214+4724 is estimated. Having established that the Balmer line flux from the INLR is very low, in Section 8 we attempt to explain the observed emission-line ratios from F10214+4742 in terms of the conventional model for Seyfert 2 galaxies. Section 9 discusses the properties of the clouds in the inner narrow-line region. Finally in Section 10 our results are summarized and some of their implications discussed.

2 NEW INFRARED SPECTROSCOPY

F10214+4724 was observed with CGS4 on the UKIRT on the nights of 1996 April 16, 17 and 18 in the *H* and *K* bands with the 150 line mm^{-1} grating, and on 1997 February 1 with the 75 line mm^{-1} grating in the *J* band as part of the UKIRT service programme. A two-pixel (2.4-arcsec) slit was used for all the observations. Spectra were taken as detailed in Table 1, and were nodded along the slit by 10 or 25 pixels in the ABBAABBA... sequence described by Eales & Rawlings (1993). This results in positive and negative object spectra appearing on the array. Various position angles were used in an attempt to detect emission lines from galaxies in the group containing the lensing galaxy.

The data were wavelength and flux calibrated in IRAF using argon or krypton arc spectra and the flux calibration standards listed in the table. A third-order polynomial fit to the columns was used to improve the subtraction of the sky lines. Additional spectra of bright stars of spectral types A, F and G were used to aid in the identification and removal of atmospheric absorption features. One-dimensional spectra were then extracted from the positive and negative traces and averaged together.

3 AN EMISSION LINE FROM THE LENSING SYSTEM?

An emission line is seen in the spectrum offset by about one pixel (1.2 arcsec) from the object spectrum at 1.256 μm (Fig. 1). This does not correspond to any known emission line at the redshift of F10214+4724, and we therefore assume it originates in the lensing system, probably in source 2 of Matthews et al. (1994), but with a possible contribution from source 3. As both sources 2 and 3 have similar spectral energy distributions in the optical, which we identified with galaxies at $z \approx 0.9$ in Paper I, we have identified the emission line as Hα at $z = 0.914$. This is slightly different from the absorption line redshift of 0.893 tentatively obtained by Goodrich et al. (1996), but this may be a result either of errors in identifying and measuring these weak features (see discussion in

Table 1. CGS4 observations of F10214+4724.

Date	Central wavelength /μm	Grating	Grating order	PA /deg	Integration time /minutes	Flux standard and magnitude
16/04/96	2.265	150 l/mm	1	90	64	HD 105601 ($K = 6.69$)
16/04/96	2.265	150 l/mm	1	0	128	HD 105601 ($K = 6.69$)
17/04/96	1.580	150 l/mm	2	50	64	BS 4039 ($H = 4.52$)
17/04/96	1.580	150 l/mm	2	22	64	BS 4039 ($H = 4.52$)
18/04/96	2.140	150 l/mm	2	90	96	BS 4030 ($K = 4.40$)
01/02/97	1.220	75 l/mm	2	22	96	BS 4051 ($J = 5.58$)

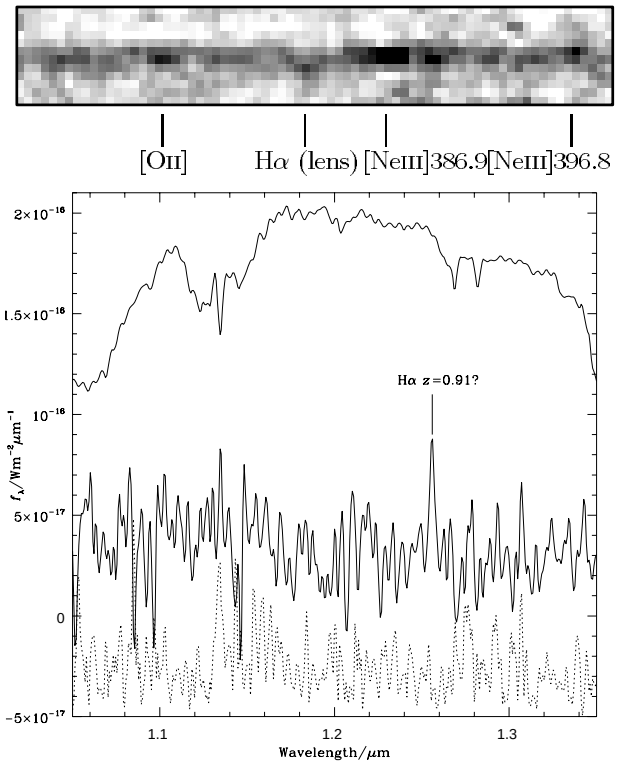

Figure 1. Top: grey-scale of part of our J-band spectrum of F10214+4724 showing the candidate emission line from the lens and the [O II] and [Ne III] emission lines from the object. Bottom: the J-band spectrum extracted ≈2 arcsec along the slit showing the emission line from the lensing galaxy (lower solid curve). Lower curve (dotted): noise estimate from the mean of three extractions of sky near to the object, displaced by -5.0×10^{-17} W m^{-2} μm^{-1}. Upper curve: relative atmospheric transmission as a function of wavelength, multiplied by 2.0×10^{-16} W m^{-2} μm^{-1} .

Section 7), or of one redshift being that of source 2 and the other being that of source 3. If so, this gives a velocity difference of 3300 km s^{-1}, large for a galaxy group but possibly consistent with sources 2 and 3 being members of the same galaxy cluster.

4 THE BALMER LINES FROM F10214+4724

Inspection of the Hα/[N II] blend at our highest resolution (FWHM of 0.0012 μm, or a resolving power of 1800) reveals a complicated structure, rendered more so by a bright sky line at 2.1518 μm, the OH^- Q transition (Ramsay, Mountain & Geballe 1992) which is saturated in our spectrum, and is coincident with the [N II] 654.8 line. Nevertheless, it seems clear that the [N II] 658.4 line has a width consistent with the rest of the emission from the INLR, i.e. about 1000 km s^{-1}, whereas the Hα line has a component which is significantly narrower. We therefore attempted a χ^2 fit to the data with eight free parameters: a constant continuum level, a wavelength, flux and width for the [N II] 658.4 line (the properties of the [N II] 654.8 line are then fixed as the ratio [N II] 658.4/[N II] 654.8 = 3), a wavelength, flux and width for the narrow component of Hα, and finally a flux for the component of Hα which has the same width and redshift as the [N II] emission. The region of the saturated sky line was excluded from the fit, as was the part of the spectrum around 2.178 μm which was struck by a cosmic ray. The results of this fit are given in Table 2, and in Fig. 2 the results are plotted and compared to the data.

We found that small changes in, e.g., the details of extraction and

Table 2. Results of a fit to the Hα/[N II] blend.

Line	wavelength /μm	redshift	flux /10^{-19} Wm^{-2}	FWHM /km s^{-1}
[NII]658.4	**2.1642**	2.2871	**28**	**1000**
Hα SF	**2.1576**	2.2875	**8.2**	**220**
Hα INLR	2.1507	2.2871	**1.0**	1000

Notes: items in bold face were free parameters in the model (see text).

removal of bad pixels resulted in a large range in the flux of the Hα component from the INLR (the flux of this component is probably only accurate to about a factor of three), but the basic results, namely that the [N II] lines are dominated by a component similar in width to the narrow lines in the optical spectrum, whereas the Hα emission is dominated by a significantly narrower (FWHM ≈220 km s^{-1}) component seem robust. The closeness of the FWHM of the narrow Hα component to that of the CO 3-2 line (Radford et al. 1996) make it tempting to identify the narrow Hα emission line with star-forming activity (cf. Paper II).

Comparison of our results with previous attempts at deblending the Hα/[N II] complex (Elston et al. 1994; Kroker et al. 1996; Paper II) make it clear that the high spectral resolution is required to detect the narrower Hα component. In common with Elston et al. (1994) and Paper II but at variance with Kroker et al. (1996) we find no evidence of an Hα component from the broad-line region. Comparing with Paper II, we find that our higher resolution spectrum shows that the [N II] 658.4 line is dominated by the INLR component, and the contribution of any narrow component associated with the star-forming region to the [N II] flux must be small. As a consequence, we find that the Hα flux from the INLR is much smaller than that

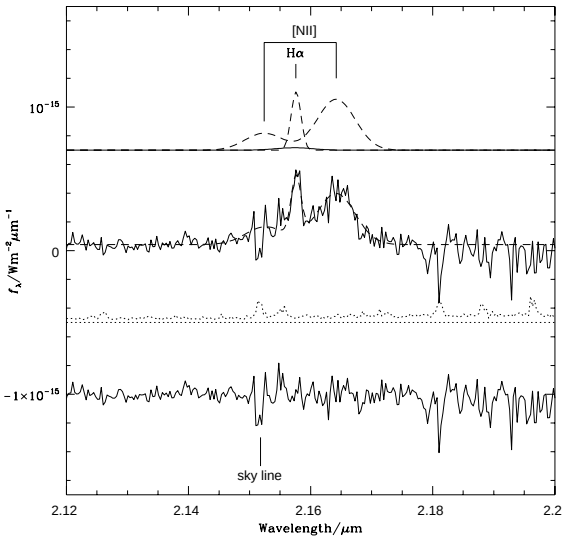

Figure 2. The Hα/[N II] blend and its fit. The top set of lines show the emission-line component fit to the blend. The [N II] and narrow Hα components are shown dashed, the broader 'INLR' Hα component is the solid line. The next set of lines down are the data themselves, with the fit plotted through them as a dashed line, including the continuum level of 4.2×10^{-17} W m^{-2} μm^{-1} ($K\approx17.5$). The dotted line below this is the noise as a function of wavelength that was used in the χ^2 fit. The bottom solid line is the residual from the fit. The position of a strong sky line near the weaker of the [N II] doublet is indicated.

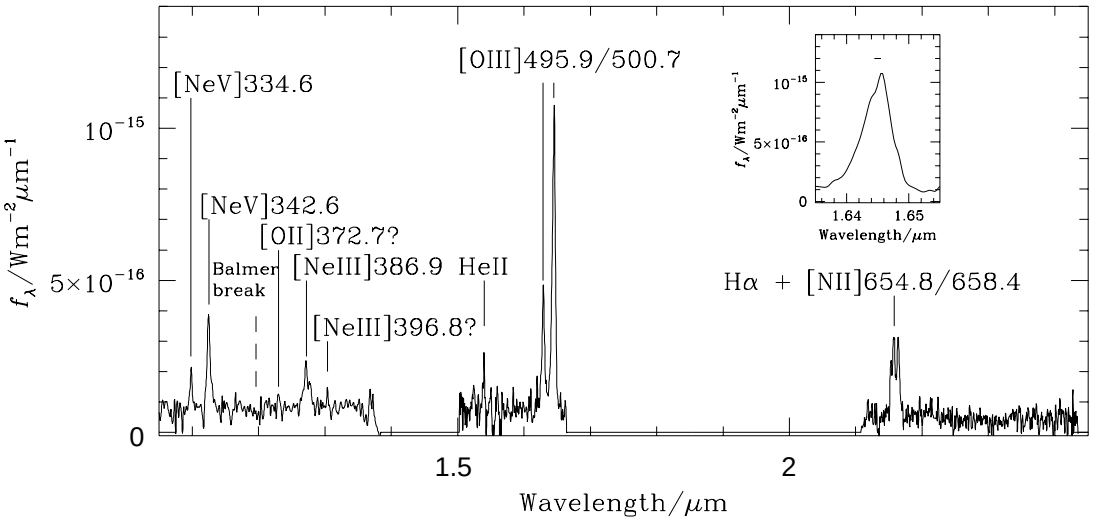

Figure 3. The near-infrared spectrum of F10214+4724. The *J*- and *K*-band spectra have been smoothed with a three-pixel smoothing box, the *H*-band spectrum (at higher resolution originally) has been smoothed twice. The position of the Balmer break is indicated. Inset: detail of the [O III] 500.7 line showing the blue wing; the FWHM of the instrumental profile is shown as a bar centred on the peak of the line.

estimated in Paper II, with most of the flux in the Hα+[N II] complex coming from the INLR component of [N II].

To obtain upper limits on the fluxes of Hα lines from the broad-line region (BLR), we have added in an artificial broad component to the first order *K*-band spectrum. To begin with, we assumed an FWHM of 10 000 km s^{-1} for the broad line, based on the Keck spectrapolarimetry of Goodrich et al. (1996) who measure this width for the broad component of the C III 190.9 line. Our limit on the broad Hα flux from this was obtained from the first order *K*-band spectrum to be $\approx 5\times10^{-18}$ W m^{-2}, corresponding to a signal to noise ratio of about 2σ per resolution element at half maximum intensity. We also tried a 4000 km s^{-1} FWHM line, the broad C III] linewidth measured in direct light in Paper II. We have placed a similarly derived limit of $\approx 2\times10^{-18}$ W m^{-2} on the flux of such a component. This compares with the claimed detection of a broad line with a flux of $\approx 3.7\times10^{-18}$ W m^{-2} and a width of 2400 km s^{-1} by Kroker et al. (1996), which on the basis of these calculations we should have easily detected.

5 THE *J*- AND *H*-BAND SPECTRA

Fig. 3 shows the *J*-, *H*- and first-order *K*-band spectra (Table 3) which between them cover most of the available near-infrared window.

In the *J* band, the [Ne v] 334.6 and 342.6 lines are clearly detected, along with the [Ne III] 386.9 line. Marginally detected are the [O II] 372.7 and [Ne III] 396.8 lines (see also Fig. 1). Interestingly, both our [O II] detection and that of Soifer et al. (1995) has the [O II] emission redshifted with respect to the higher ionization lines by about 500 km s^{-1}.

The *H*-band spectrum shows a clearly detected and resolved [O III] doublet, and a marginal detection of He II 468.6. There is no detection of Hβ to a limit of $\approx 2\times10^{-19}$ W m^{-2}.

These spectra are consistent with earlier observations at lower spectral resolution (Soifer et al. 1995; Iwamuro et al. 1995; Paper II), and confirm the low [O II] 372.7 and Hβ fluxes found by other groups. The higher resolution of these observations shows that the FWHM of the lines is similar to those in the rest frame UV, i.e. $\approx$1000 km s^{-1}.

Table 3. The *J*- and *H*-band spectra.

Line	wavelength /μm	redshift	flux /10^{-19} Wm^{-2}	FWHM /km s^{-1}
[Nev]334.6	1.0982	2.2820	7.1	–
[Nev]342.6	1.1247	2.2828	18	1500
[OII]372.7	1.2301	2.3005	2	–
[NeIII]386.9	1.27237	2.2886	13	–
[NeIII]396.8	1.30419	2.2868	1	–
HeII 468.6	1.5397	2.2857	2.3	–
[OIII]495.9	1.6292	2.2854	18	810
[OIII]500.7	1.6450	2.2853	53	1040

6 THE REDDENING TOWARDS THE NARROW-LINE REGION

Our spectra all seem to be consistent with a low reddening towards the narrow-line region. Using the data from Paper II, the ratio of He II 468.6 / 164.0 is 4.3 (assuming our He II detection is real), compared to the case B value of $\approx$6.5 (Osterbrock 1989). This corresponds to an $A_V \approx 0.3$ if the reddening occurs in the source, much lower than the estimate of Soifer et al. (1995) ($A_V \approx 1.1$) because of our lower He II 468.6 flux measurement. Inspection of the spectrum of Soifer et al. (1995) suggests that the reason for this is a poor continuum level determination in their low-resolution spectrum. Our reddening estimate is consistent with that derived from the UV He II 108.6: He II 164.0 line ratio in Paper II.

7 THE FC2 COMPONENT

On the basis of their spectropolarimetry, Goodrich et al. (1996) have argued for the presence of an unpolarized FC2 component in the UV spectrum of F10214+4724 with a redder slope than the polarized emission and which contributes about half the UV flux. To investigate the nature of this component we examined our William Herschel Telescope spectrum (Paper II) for UV absorption features. This spectrum is shown in Fig. 4, scaled so as to show up the details of the continuum (the emission lines are discussed in Paper II). Lists

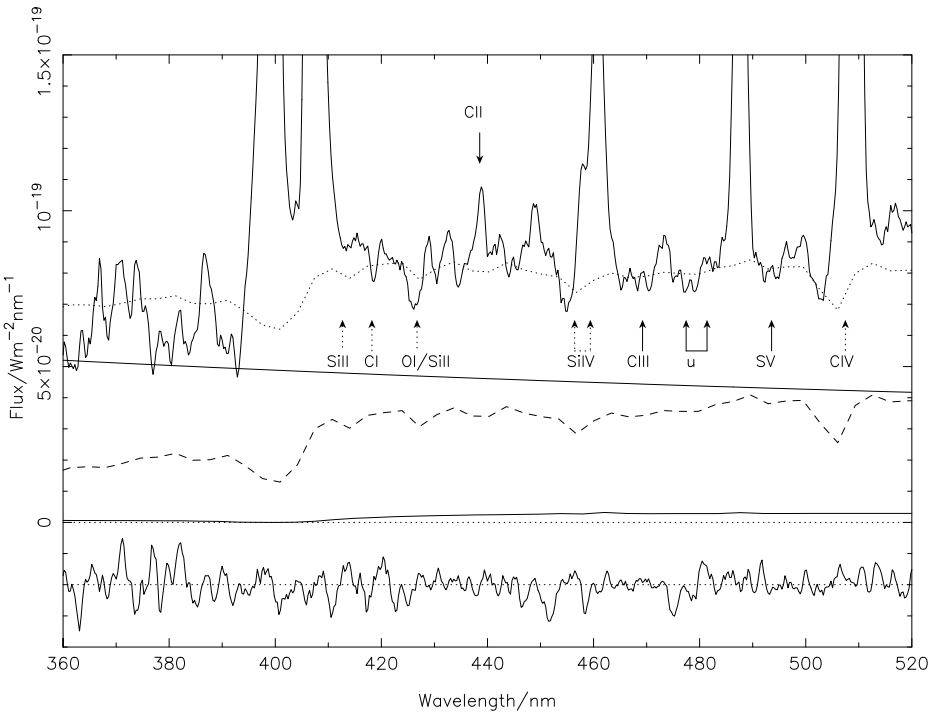

Figure 4. The UV spectrum of F10214+4724 from Paper II smoothed with a 5-pixel (1.4 nm) box-car filter. Positions of interstellar (dotted) and stellar (solid) features are indicated by arrows. Note that the arrows for the interstellar features are blueshifted by 1000 km s^{-1} relative to $z = 2.286$. The smooth solid line below the spectrum is the power-law polarized continuum of Goodrich et al. (1996) scaled by a factor of two to allow for polarization dilution. The dashed line is the starburst spectrum and the solid line below it the nebular continuum contribution. The sum of these components is the dotted line plotted through the spectrum. A noise spectrum is plotted at the bottom, displaced by -2.0×10^{-20} W m^{-2} nm^{-1}.

of interstellar and stellar absorption features from Verner, Barthel & Tytler (1994), Kinney et al. (1993) and Dey et al. (1997) were used.

The strong interstellar line blend of O I 130.2/Si II 130.4 and the stellar wind or interstellar Si IV 139.4/140.3 lines are convincingly detected. C II 133.5 is also seen in emission. All these features are also visible in the Keck spectrum of Goodrich et al. (1996).

Less convincingly detected are interstellar lines of C I 127.7 and the interstellar/stellar wind C IV 154.8/155.1 lines in absorption. Finally, much less convincing are the interstellar Si II 126.0 line and some stellar features. These stellar features are identifiable as such because they do not correspond to transitions to or from the ground state. C III 142.8, an unidentified pair of lines at 145.3 and 146.5, and S V 150.2 are all very marginally detected. The shape of the spectrum and position of the candidate absorption features are, however, consistent with the spectrum of Goodrich et al. (1996). We also note the possibility that the absorption features around 530 nm, noted by Goodrich et al. and attributed to Mg II at $z = 0.892$, may also correspond to a blend of stellar absorption features at 160–163 nm in the linelist of Kinney et al. (1993). This may also help to account for the apparent discrepancy in the emission and absorption-line redshifts for the lens. The reality of these stellar absorption features is hard to establish, as their signal-to-noise ratio is low, and the true continuum level is hard to define because of the possibility of confusion by unidentified emission lines associated with the AGN activity. We cannot thus claim to have found definitive evidence for a young stellar population, but the similarity between this spectrum and those of high-redshift starburst galaxies identified through Lyman dropout techniques (e.g. Lowenthal et al. 1997) is strong once the mostly AGN-powered emission lines are subtracted.

The absorption troughs of the interstellar and stellar wind lines are all blueshifted with respect to the mean emission line redshift of 2.286. The deepest interstellar line, that of the O I/Si II blend is blueshifted by $\approx 1200 - 1700$ km s^{-1} (depending on which of the lines dominates the blend), indicative of a rapid outflow of low ionization gas. The Si IV and C IV stellar wind absorption troughs are even more highly blueshifted, by up to 4000 km s^{-1}, as expected if they arise in supergiant winds partly filled in by the AGN emission lines. In contrast, C II 133.5 is seen in emission at the emission-line redshift, although there is a hint of absorption in the blue wing, resulting in a P-Cygni profile. Blueshifting of the interstellar absorption lines is seen in both low and high redshift starbursts (Heckman 1998), and it seems plausible that the blueshifts of the interstellar lines are the result of fast winds or superwinds from the starburst region.

To estimate the star formation rate (SFR) required to produce the FC2 component, we have used a population synthesis model from the PEGASE data base of Fioc & Rocca-Volmerange (1997) and the starburst reddening law of Calzetti, Kinney & Storchi-Bergmann (1994). The attenuation was calculated from the reddening law according to the prescription of Meurer et al. (1995). To estimate the contribution of the scattered nuclear light (the FC1 component) we take the mean polarization of the broad emission lines of Goodrich et al. (1996) to be 50 per cent. We then assume these are purely scattered light and correct the polarized continuum by a factor of two to make a rough correction for polarization dilution of the FC1. We also assume that the star formation rate has been roughly constant for $\gtrsim 10^7$yr so that the age of the starburst is longer than the lifetimes of the stars dominating the UV continuum. The reddening can then be estimated by requiring that the shape of the UV emission matches that observed. In this 'steady state' approximation we derive an SFR, corrected for a reddening of $E(B-V) \approx 0.6$ towards the continuum, of $\approx 8000\,\mathrm{M}_\odot\, m^{-1}$ yr^{-1} for

a Scalo (1986) IMF or $\approx 4000\,M_\odot\,m^{-1}\,yr^{-1}$ for a Salpeter (1955) IMF, where m is the magnification of the star-forming region.

If we identify the kinematically distinct (and spatially distinct, according to Kroker et al. 1996) narrow ($220\,km\,s^{-1}$) Hα line with star formation we can attempt to place an independent constraint on the star formation rate in F10214+4724 from this. The reddening estimate here depends on the Hα:Hβ flux ratio, and a convincing detection of Hβ has yet to be made. Nevertheless, the lowest limit, that of Elston et al. (1994), and the lower error bar on the claimed detection of Iwamuro et al. (1995) are both consistent with a flux of $\approx 10^{-19}\,W\,m^{-2}$. If we assume this value for the flux of the Hβ line then the Hα:Hβ ratio is about 9 (albeit with a high uncertainty arising from the difficulty in accurately deblending the Hα+[N II] lines), corresponding to a rest frame $E(B-V) \approx 0.9$, and hence an extinction to Hα of a factor of $\approx$7.5, assuming a case B value of 2.87 for the intrinsic Hα/Hβ ratio. Note that this is probably consistent with the lower value of reddening found for the UV flux: Calzetti et al. (1994) find that the reddening seen towards the Balmer emission lines is typically greater than that seen towards the continuum in nearby starbursts, perhaps because the very massive stars producing the bulk of the ionizing radiation are too short-lived to escape from the dusty regions in which they are formed. With this amount of reddening any [O II] 372.7 emission from the starburst would be undetectable in our spectrum.

The star formation rate from the Hα luminosity in the starburst component can be compared to the value predicted from the UV star formation rate: for a Scalo IMF, Gallego et al. (1995) obtain a conversion of Hα luminosity to star formation rate of 0.94×10^{34} $W\,M_\odot^{-1}yr$, and for a Salpeter IMF Bunker (1996) obtains 3.108×10^{34} $W\,M_\odot^{-1}yr$. These give star formation rates of 2550 and 740 $M_\odot\,m^{-1}\,yr^{-1}$ for Scalo and Salpeter IMFs respectively, corrected for reddening, lower than those obtained from the UV. Given the large uncertainties in the estimates of the star formation rate from the two different methods though, their agreement to within an order of magnitude is probably as good as can be expected.

It is clear from the *HST I*-band image of Eisenhardt et al. (1996) and from the *B*-band image of Broadhurst & Lehar (1995) that the UV continuum is dominated by the $\approx$0.7-arcsec arc of highly magnified emission. In contrast, about 30 per cent of the narrow Hα emission is seen to be extended over $\approx$2 arcsec according to Kroker et al. (1996). Thus it is plausible that some ionizing radiation escapes from the star-forming region to ionize gas further out, which may itself have been expelled from the nucleus in a 'superwind', or may be infalling; emission from this gas will less magnified (the magnification scales approximately with the inverse of the size of the emission region). This gas could of course equally well be ionized by the AGN, however.

We can further compare these estimates to models for the far-infrared emission. A limit on the size of any starburst region can be estimated from the size of the radio source, which is approximately the same as that of the bright UV source, as one would expect if a large fraction of the UV was from star formation. Green & Rowan-Robinson (1996) show that, for a starburst to fit within the radio source scale-size requires a high optical depth ($\tau_{UV} \approx 800$) model with several starburst clouds along the line of sight. Such a model contributes $\approx$40 per cent of the infrared luminosity, $\approx 2 \times 10^{14}\,L_\odot$. Using the conversion of infrared flux to SFR of Condon (1992) implies an SFR $\sim 20\,000\,M_\odot\,m^{-1}\,yr^{-1}$ for stars $> 5\,M_\odot$, or a total of $\sim 10^5\,M_\odot\,m^{-1}\,yr^{-1}$ assuming a Salpeter IMF. This is 1–2 orders of magnitude higher than deduced from the UV and Hα emission, but the high optical depths necessary in the model to keep the source size small would certainly imply that the bulk of the star formation would be hidden. Further evidence that much of the starburst could be hidden comes from Kroker et al. (1996), who suggest that the reddening derived from Hα could be an underestimate as the CO fluxes from F10214+4724 convert to $A_V \geq 100$ assuming galactic gas:dust conversion factors.

The exact value of the magnification of the starburst region is controversial. As Trentham (1995) shows, the probability of obtaining a high magnification is strongly dependent on the source size. He demonstrated that a magnification factor of $\gg$10 was very unlikely if the source size was $\sim$1 kpc or larger. Smaller sources could, however, be much more highly magnified. Other arguments in favour of small magnifications ($m \sim 10$) come from the size of the CO emission region, which is marginally resolved by Downes, Solomon & Radford (1995) with a size of $1.5 \pm 0.4 \times \leq 0.9$ arcsec^2, and modelling of the far-infrared flux (e.g. Green & Rowan-Robinson 1996). The larger size of the near-infrared arc (2 arcsec) has also lead to suggestions that this corresponds to the dusty starburst region, which would have an unmagnified size of $\approx$1 kpc (Graham & Liu 1995). The radio source and the UV source are, however, the same size (within the errors) and this size ($0.7 \times \leq 0.1$ arcsec^2), combined with the lens models, suggests higher values, $m \sim 50-100$ corresponding to source sizes of $\sim 40-80$ pc (Broadhurst & Lehar 1995; Eisenhardt et al. 1996) if the radio source is associated with the starburst.

The minimum size for the infrared source based on blackbody arguments provides another constraint. Using an effective temperature of 140 K, corresponding to the peak in the observed mid-infrared flux, Eisenhardt et al. (1996) estimate this minimum size to be 130 pc, corresponding to $m = 42$. This small source size was assumed by Broadhurst & Lehár (1995) to prove an AGN origin for the far-infrared emission, but compact starbursts may be common in infrared-luminous galaxies. For example, the radio supernovae in the northeastern component of Arp 220 are contained within a projected area of only 100×200 pc^2 (Smith et al. 1998).

There is nevertheless a factor of $\approx$2 difference between the best estimate of the UV magnification and the maximum IR magnification from the blackbody argument. This could arise for several reasons. First, the starburst may simply be smaller than the IR black-body size, giving a small radio/UV source with high magnification. This is, however, statistically unlikely as it requires the starburst to be well-centred on the cusp, even though, provided some part of the infrared source lies on the cusp, the infrared magnification will not depend strongly on the exact position relative to the cusp. Alternatively, the starburst size may be comparable to the blackbody size, but patchy extinction may lead to clumpy UV emission. If one of these clumps falls on the cusp it will be strongly magnified relative to the bulk of the infrared flux. The similar lengths of the radio and UV arcs need not rule this out: if the UV-emitting region is offset towards the edge of the infrared source, the lengths of the UV and radio arcs could be similar, but the magnifications different. Close to the caustic $m \propto b^{-1}$, where b is the impact parameter (Broadhurst & Lehár 1995). Thus the length of the arc $l \propto mr \approx$ constant if $b \approx r$, where r is the size of the source. This hypothesis can be tested with a detailed comparison of the *HST* and deep, high-resolution radio images which should show small differences in the structure of the arc between radio and UV wavelengths. Lens modelling uncertainties and uncertainty in the precise wavelength of the mid-infrared peak may also help to account for the difference in the magnifications.

To summarize: from our near-infrared studies we can place a fairly conservative lower limit on the SFR in F10214+4724 of

$\gtrsim 10\, m_{100}^{-1}\, M_\odot\, yr^{-1}$ where m_{100} is the magnification of the UV/optical arc in units of 100. This is consistent with the FC2 component being entirely produced by star formation, as is suggested by the similarity of the spectral features in the UV to those seen in starburst galaxies. Our data are also consistent with much higher star formation rates if the bulk of the star formation is hidden by dust, up to the $\sim 2.5 \times 10^3 (m_{FIR}/40)^{-1}\, M_\odot\, yr^{-1}$ estimated from the far-infrared flux, where m_{FIR} is the magnification of the far-infrared flux. The unobscured starburst region is compact, with a scale size $\sim$100 pc. High-velocity winds are present in the interstellar gas. It is therefore likely that, as suggested in the case of Mrk 477 by Heckman et al. (1997), the star formation is taking place in the outer regions of the obscuring torus, where conditions in the gas (which is sufficiently distant from the AGN to be shielded from its radiation field by the inner torus) are likely to support star formation.

8 THE EMISSION-LINE RATIOS

The unusually weak [O II] 372.7 and Balmer lines have been a particular problem in explaining the emission-line properties of F10214+4724. Rather than attempt to model the emission-line ratios using a photoionization code, as attempted by Soifer et al. (1995) and by ourselves in Paper II, in this paper we have adopted a more empirical approach. Table 4 compares the emission-line ratios of F10214+4724 with those of the nearby Seyfert 2 galaxy NGC1068, normalized to He II 164.0. As can be seen, the line ratios are remarkably similar, including the He II reddening diagnostic lines (108.5, 164.0 and 468.6 nm) even with no attempt at dereddening the spectra (which in the case of NGC1068 at least is complicated by apparently wavelength-dependent extinction corrections, cf. Ferguson, Ferland & Pradhan 1995, and/or possible blending of the He II 108.5 line, e.g. Netzer 1997). The strong UV lines (e.g. O VI, N V, C IV, C III]) are all well-reproduced. Many of the optical line ratios are also very similar to within a factor of two (e.g. [Ne III], [O III] 500.7) with the exception of the hydrogen lines, and lines having critical densities $n_{crit} \lesssim 10^{10}\, m^{-3}$ ([O II] 372.7, [S II] 671.7/673.1) which are suppressed by factors $\approx$6. Lines with $n_{crit} \sim 10^{11-12}\, m^{-3}$ ([N II] 654.8/658.4, [O III] 495.9/500.7) are low by factors $\approx$2, but not very discrepant given the typical range in line ratios (Simpson & Ward 1996) and the uncertainty in the differential reddening between the two objects. [Ne V] 342.6 is higher in F10214+4724 by a factor of $\approx$3, but there is a general trend for all the Ne lines to be brighter than their counterparts in NGC1068, and so it may be at least partly accounted for by an enhanced Ne abundance relative to NGC1068.

On this basis it seems likely that the low n_{crit} lines are being suppressed because the nebular density in a typical cloud, n, is relatively high, $\sim 10^{10-11}\, m^{-3}$. This most likely results from the fact that lensing is preferentially magnifying the INLR, where the cloud densities are higher than the mean for the narrow-line region . In the Simpson & Ward (1996) model, the cloud densities are $\propto r^{-2}$ where r is the distance from the nucleus. The ionization parameter is therefore independent of the distance from the nucleus, which helps to explain why magnification of the INLR has not produced a much higher ionization spectrum than that for normal luminous Seyfert 2s.

This interpretation is supported by the *HST* spectrum of NGC1068 taken by Caganoff et al. (1991) using a 0.3-arcsec ($\approx$30 pc) aperture centred on the UV continuum peak. Although few line fluxes are given in the paper, we have attempted to measure line ratios from their plot. Within this small aperture, the degree of ionization as measured by the [Ne V] 342.6:[Ne III] 368.9 ratio seems higher than in our spectrum of F10214+4724 (1.8 compared to 1.3) and also higher than in the wide aperture (2.7×4.0 arcsec^2) spectrum of NGC1068 in Table 4 (0.8), which contains a factor of 9.4 more Hβ flux. This suggests a departure from the $n \propto r^{-2}$ law, in the sense that the density is decreasing more slowly with radius than r^{-2}. Nevertheless, a change in the [Ne V] 342.6:[Ne III] 368.9 ratio of only a factor of 2.3 in an order of magnitude difference in aperture size suggests that the approximation of constant U with radius is probably not too bad.

The Caganoff et al. spectrum has weaker [O II] 372.7 and [S II] 671.6/673.2 emission relative to He II 468.6 than for the NGC1068 spectrum through the larger aperture by factors of $\approx$2 and 4 respectively, and also a weaker Hβ line by a factor of $\approx$2. From the [O II] doublet ratio, Caganoff et al. estimate $n \approx 1.2 \times 10^9\, m^{-3}$, about an order of magnitude less than we estimate for F10214+4724, and this seems consistent with a less dramatic suppression of the low n_{crit} and Balmer lines in the INLR of NGC1068 than in that of F10214+4724, despite the higher ionization of the small aperture NGC1068 spectrum.

Table 4. A comparison of the emission line ratios of F10214+4724 and NGC 1068.

Line	F10214+4724 (raw)	NCG1068 (raw)	F10214+4724 dereddened
OVI 103.2	0.45	0.76	0.87
OVI 103.8	0.43	0.99	0.82
HeII 108.5	0.14	0.17	0.23
CIII 117.6	0.04	$\leq$0.07	0.06
Lyα	1.0	4.8	1.3
NV 124.0	1.4	1.3	1.8
CII 133.5	0.03	0.16	0.03
SiIV 139.4 +OIV 140.3	0.40	0.41	0.44
NIV 148.7	0.40	0.24	0.42
CIV 154.9	1.9	1.9	1.9
[NeIV] 160.2	0.11	$\leq$0.07	0.11
HeII 164.0	1	1	1
[OIII]166.5	$\leq$0.05	$\leq$0.07	$\leq$0.05
NIII]175.0	0.20	0.27	0.20
MgVI 180.6	0.15	0.09	0.15
CIII]190.9	0.65	1.12	0.65
[NaV] 206.7	0.12	0.05	0.14
NII]214.3	0.08	0.07	0.10
CII]232.6	0.30	0.25	0.32
[NeIV]242.2	0.52	0.40	0.51
[NeV]342.6	1.50	0.54	1.16
[OII]372.7	0.09	0.57	0.07
[NeIII]386.9	1.13	0.70	0.84
HeII 468.6	0.23	0.29	0.16
Hβ	$\leq$0.1	0.75	$\leq$0.07
[OIII]500.7	5.0	9.9	3.4
[OI]630.0	0.18	0.46	0.11
Hα	$\sim$0.1	3.35	$\sim$ 0.06
[NII]658.4	2.8	6.0	1.7
[SII]671.7/3.2	0.17	1.10	0.10
[ArIII]713.6	0.12	0.33	0.07
[OII]732.5	0.23	0.26	0.14

Note: Line fluxes are normalized to He II 164.0. The reddening assumed for F10214+4724 is $E(B-V) = 0.1$, and a standard galactic reddening curve (Cardelli, Clayton & Mathis 1989) assumed. Emission line fluxes for NGC1068 are from Kriss et al. (1992); Antonucci, Hurt & Miller (1994); Snijders, Netzer & Boksenberg (1986); Koski (1978), and Osterbrock & Fulbright (1996).

We can probably rule out the alternative possibility, i.e. that the lower ionization lines are suppressed as a result of their being formed at the edge of the narrow-line clouds and therefore not being lensed by as large a factor. As discussed in Section 7, magnification near a caustic $\sim b^{-1}$. The INLR is $\gtrsim$10 pc from the nucleus, very large compared with the thickness of the ionized layer, only $\sim 10^{15}$ m for a density $n \sim 10^{10.5}\,\mathrm{m}^{-3}$. Thus differential magnification of the ionization structure of individual clouds is unlikely to affect the observed line ratios.

The low levels of the H lines present a bigger problem. In Paper II we discussed the possibility of suppressing Lyα through resonant scattering in an H I column, and used the velocity splitting of the Lyα components to estimate the column density. In this paper we have further shown that both the Hα and Hβ fluxes from the INLR are very weak, resolving the problem of having discrepant reddening estimates from the H and He lines, but we still need to explain the general weakness of the Balmer lines. We now consider three possibilities to help explain the lack of Balmer lines: (i) the Balmer lines are optically thick, (ii) the Balmer lines are weakened by underlying absorption, and (iii) the INLR has a very high metallicity. Possibility (ii) can probably be completely discounted as we see no Balmer break in either our J-band spectrum or that of Soifer et al. (1995). Possibility (iii) can probably also be ruled out as we would not expect to see the He II:metal emission line ratios to be so similar to those in NGC1068, which has much brighter H lines. This leaves the optical thickness of the Balmer lines as the only remaining explanation. As we now show, it seems plausible as the Balmer line optical depth is indeed significant. Davidson & Netzer (1979) show that the optical depth to Hα is given by

$$\tau_{\mathrm{H}\alpha} \approx \sigma_{\mathrm{H}\alpha} A_{\mathrm{Ly}\alpha}^{-1} \zeta F_{\mathrm{H}} K_1 \tau_{\mathrm{Ly}\alpha},$$

where $\sigma_{\mathrm{H}\alpha} = 10^{-16.4}\,\mathrm{m}^2$ at the line centre is the cross-section of the $n = 2$ state to an Hα photon, ζ and K_1 are factors of order unity, F_{H} is the flux of ionizing photons, $\tau_{\mathrm{Ly}\alpha}$ is the optical depth to the Lyα line and $A_{\mathrm{Ly}\alpha} = 4.7 \times 10^8\,\mathrm{s}^{-1}$ is the Einstein A-coefficient of the $2p$ state. Assuming a dimensionless ionization parameter $U = 0.1$ and a hydrogen density $n = 10^{10.5}\,\mathrm{m}^{-3}$ gives $F = cnU = 9 \times 10^{17}\,\mathrm{m}^{-2}\,\mathrm{s}^{-1}$, so $\tau_{\mathrm{H}\alpha} \sim 10^{-7}\,\tau_{\mathrm{Ly}\alpha}$.

According to Paper II, the minimum column density in H I required to produce the observed Lyα profile is $2.5 \times 10^{25}\,\mathrm{m}^2$, which, assuming a cross-section to the line centre of Lyα of $4.5 \times 10^{-18}\,\mathrm{m}^2$ gives $\tau_{\mathrm{Ly}\alpha} \gtrsim 1 \times 10^8$ to the line centre. Thus $\tau_{\mathrm{H}\alpha} \gtrsim 10$.

As Ferland & Netzer (1979) point out, however, this estimate of the optical depth needs to be interpreted carefully. Most of the optical depth arises in the partially ionized region of the nebula, where the Lyα photons are being resonantly scattered and the population of the $n = 2$ level is therefore highest. Provided the cloud is radiation-bounded, escape of Hα photons from the illuminated side of the nebula is far more likely than escape from the non-illuminated side (as is also the case for Lyα photons). Thus if we are observing the clouds from the non-illuminated side, we expect the Balmer and Lyα lines to be substantially suppressed. This case is therefore different from that for the UV resonance lines, e.g. O VI and C IV, which may also be optically thick in F1024+4724 (Paper II). In the cases of these lines, there are no reflecting layers to backscatter the photons: provided they are not absorbed by dust they will eventually escape isotropically.

The lack of hydrogen lines in F10214+4724 can thus be explained as a geometrical effect. Back-scattering of the Balmer and Lyα lines in the INLR suppresses them relative to the outer narrow-line region, where escape is easier. This effect will be most pronounced if the side of the INLR which is closest to the cusp in the lensing potential is between us and the AGN (Fig. 5). In this geometry, we see the back sides of the most highly magnified narrow-line clouds, through which little flux from H lines can escape. Heisler, Lumsden & Bailey (1996) show that polarized broad lines are only detected in Seyfert 2 galaxies the torus axes of which are inclined relatively close to the angle at which the BLR becomes visible, thought to be about 45 deg. Inclination at such an angle will also improve suppression of the H lines in our back-scattering model.

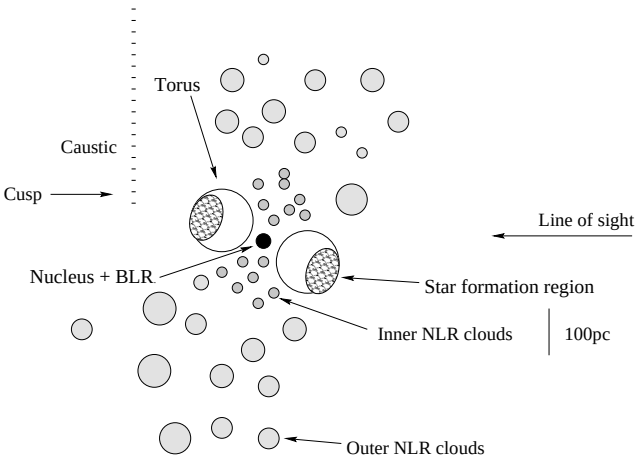

Figure 5. The geometry required to produce the observed emission line properties of F10214+4724. The line marked 'caustic' indicates the line of the caustic in the lensing potential, which reaches a cusp close to the nucleus and just above it (see fig. 1 of Broadhurst & Lehár 1995), thus preferentially magnifying the forward-pointing side of the ionisation cone.

In a normal Seyfert 2 such as NGC1068, we see brighter H lines because the outer narrow-line region is optically thin to Hα, thus enabling us to see the Balmer lines from the near side, and the contribution from the far side of the central object is larger, allowing both Lyα and Balmer lines to be seen from there. It is also likely that apart from lensing, obscuration by the dusty molecular torus of the other side of the INLR helps to reduce the Balmer and Lyα contributions from the far side of the central object. Partial obscuration of the INLR has been used to explain the differences in [O III] emission line strengths between quasars and radio galaxies (Hes, Barthel & Fosbury 1993).

9 INFERRED PROPERTIES OF THE INNER NARROW-LINE CLOUDS

Given an estimate of the density, ionization parameter and the neutral column, we can attempt to deduce the typical sizes and masses of the narrow-line clouds. The ionized column N_{H^+} can be estimated from the ionization parameter, density and ionizing flux from

$$N_{\mathrm{H}^+} = \frac{Uc}{\alpha_{\mathrm{B}}} \approx 1 \times 10^{26}\,\mathrm{m}^{-2}$$

where $\alpha_{\mathrm{B}} = 2.58 \times 10^{-19}\,\mathrm{m}^3\,\mathrm{s}^{-1}$ is the case B recombination coefficient. To this, the neutral column adds a comparable $\approx 2.5 \times 10^{25}\,\mathrm{m}^{-2}$ (Paper II). Hence assuming a uniform density cloud, a typical size is $\sim$0.1 pc and a typical mass is $\sim 1\,\mathrm{M}_\odot$, a little larger than the estimates in Paper II because of our inclusion of the ionized column.

We can compare our results to the theoretical predictions of

Mathews & Veilleux (1989) who deduced from a stability analysis of the clouds in the narrow-line region an $N_{\rm H} \sim 10^{26} - 10^{28}\,{\rm m}^{-2}$. Clouds in outflowing winds with column densities in this regime are stable to Rayleigh–Taylor instabilities when radiative pressure and dynamical pressure act together, yet are small enough both to ensure a covering factor << 1 and smooth line profiles.

Extinction by dust in the inner narrow-line clouds would be expected to affect the observed line ratios, particularly if, as our model predicts, we are seeing emission-line light emerging through large column densities in the narrow-line clouds. From our derived column density (ionized plus neutral) and assuming a gas:dust ratio of $N_{\rm H}/E(B-V) = 4.5 \times 10^{25}\,{\rm m}^{-2}\,{\rm mag}^{-1}$ (Bohlin, Savage & Drake 1978), we obtain $E(B-V) \approx 2.8$ mag, much larger that the $\approx$0.1 we measure (which of course is an upper limit to the amount of reddening within the narrow-line clouds, as it does not include dust outside the nuclear region). The double Lyα line is also good evidence against dust in the neutral column, as even a small amount of dust would destroy Lyα photons. Thus the narrow-line clouds must contain relatively low amounts of dust. Even at 10 pc from the AGN, we are well away from the dust sublimation point, thought to be just outside the broad-line region (Laor & Draine 1993). The narrow-line clouds may start their lives close to the AGN and then flow out, or perhaps have their dust destroyed by shocks associated with the AGN.

Our column depths are also consistent with models in which the fully-ionized 'warm absorbers' seen in the X-ray spectra of Seyfert 1 galaxies and quasars, and possibly related to associated absorbers seen in quasar spectra, are narrow-line clouds seen close to the nucleus (e.g. George et al. 1998). These have typical column densities $\sim 10^{25} - 10^{27}\,{\rm m}^{-2}$, but seem to be mostly dust free, and this, coupled with their short variability timescales, suggests an origin at least as close to the AGN as the outer broad-line region. Outflow of these clouds into the narrow-line region in a decelerating flow (Crenshaw 1997) would account for the lack of dust in the inner narrow-line clouds.

9.1 X-ray emission

In common with most Seyfert 2 galaxies, the X-ray emission from F10214+4724 is weak (Lawrence et al. 1994), implying an absorbing H I column of $\sim 5 \times 10^{27}\,{\rm m}^{-2}$, an order of magnitude higher than that in our narrow-line clouds, and consistent with the absorption taking place in a torus of neutral gas around the AGN. Such a column implies a reddening $E(B-V) \sim 100$ if the gas:dust ratio is galactic, or $\lesssim$5 if it is the same as deduced from the narrow-line clouds. Either would also be more than sufficient to hide the nucleus and broad-line region in the UV and optical.

10 DISCUSSION

Our studies of IRAS F10214+4724 have allowed us to plausibly resolve many of the remaining puzzles relating to this object. Furthermore, the lensed nature of the galaxy has allowed us to examine the nuclear region in detail only achievable with the *HST* on the most nearby Seyfert galaxies. With this we have been able to argue that there is a probably an intimate link between a starburst and AGN in this object, namely that the starburst is occuring very close in to the nucleus, possibly in the obscuring torus. From optical depth arguments we have been able to deduce many of the properties of the narrow-line clouds in the INLR, and thus address some of the issues associated with absorption of AGN spectra.

Fig. 5 shows the model we have chosen to adopt for the nuclear regions of F10214+4724. This gives the greatest suppression of the hydrogen lines, although in fact any geometry in which the cusp falls in front of the INLR will lead to some suppression. The axis of the dusty molecular torus is inclined such that the cusp of the lensing potential falls on the side of the ionization cone which points towards the line of sight. This enables us to scatter the Lyman and Balmer emission from the back-side of the clouds in the highly magnified INLR. The INLR has a similar scale size ($\sim 50 - 100$pc) as the mid-infrared source needs to have if the intrinsic luminosity is to be comparable with local ultraluminous *IRAS* galaxies (Broadhurst & Lehár 1995; Eisenhardt et al. 1996), i.e. if the magnification $\sim 50 - 100$. The low-density outer part of the narrow-line region has a much lower magnification, and the other side of the INLR both has a lower magnification and may be partially obscured from our line of sight by the torus. Thus lines from the low-density clouds in the outer narrow-line region and the Balmer and Lyα lines appear anomalously weak.

10.1 The nature of the inner narrow-line clouds

Using the narrow-line spectrum, we can specify the properties of a 'typical' inner narrow-line cloud. Densities inferred from the suppression of emission lines of low $n_{\rm crit}$ are $n \sim 10^{10.5}\,{\rm m}^{-3}$, with an ionization parameter of $U \sim 0.1$ inferred from the relative strength of high-ionization lines. Column densities in ionized and neutral gas are predicted to be comparable if the double-peaked Lyα line is formed by propagation through the neutral backs of the narrow-line clouds. This is consistent with the appearance of emission from neutral oxygen in the spectrum, but requires the narrow-line clouds to have a low dust content.

Our column density estimates are consistent with the narrow-line clouds being in outflow from the nucleus, stabilized according to the mechanism of Mathews & Vielleux (1989), with an origin close to the BLR to account for their low dust content. When they are closest to the nucleus they may appear as warm absorbers in X-ray spectra.

Narrow-line profiles in AGN (including F10214+4724; see Fig. 3) almost invariably have blue wings and it has been recognized for some time that a possible explanation of this is that the clouds are outflowing, with clouds on the far side of the nucleus from the observer being partially obscured (e.g. Osterbrock 1989). The alternative, that the narrow-line clouds are infalling and dust absorption in the rear of the clouds preferentially attenuates light from the near side of the narrow-line region can, in the case of F10214+4724 at least, be ruled out.

10.2 F10214+4724 in context

The angular magnification provided by gravitational lensing of F10214+4724 has allowed us to observe the emission from within the inner 100 pc of the AGN, scales which can usually only be studied in the most nearby objects. If our model for F10214+4724 is correct, the unlensed Seyfert 2 galaxy is remarkably similar to the most luminous local examples. The detection of polarized broad lines, an associated compact starburst and nuclear radio emission all have precedents at low redshift.

F10214+4724 is seen at a redshift close to the apparent peak in star formation activity in the Universe, and has a UV component very reminiscent of the Lyman break galaxies (e.g. Lowenthal et al. 1997), although much more reddened. Once corrected for lens magnification, the star formation rate deduced from the Hα and UV fluxes is only a factor of a few to ten higher than predicted in the

average massive galaxy at these epochs, although in the case of F10214+4724 it is confined to a very small region near to the nucleus. The evidence for dust both from the Hα/Hβ line ratio and the slope of the UV spectrum is strong, however, and it is quite plausible that much of the evidence for star formation could be hidden in the UV and optical, appearing only as an infrared excess. Thus although the optical/UV evidence for a starburst in F10214+4724 is fairly convincing, on the basis of our observations alone we cannot tell which of the starburst or the AGN dominates the mid-infrared flux.

Surveys for objects like F10214+4724 are already succeeding. The *Infrared Space Observatory* study of the *Hubble Deep Field* (Rowan-Robinson et al. 1997) has found several $z \lesssim 1$ galaxies with mid-infrared excesses indicative of dust-shrouded starbursts, and recently, Ivison et al. (1998) have announced the first detection of a high-z galaxy discovered with the SCUBA submm instrument, SMM 02399-0136, discovered as part of a survey behind the galaxy cluster A370 (Smail et al. 1997). Like F10214+4724, this galaxy is a narrow-line AGN with relatively weak Lyα emission and blueshifted UV absorption features, including C IV and Si IV, and possibly Si II152.7 (although this looks more likely to be part of a broad absorption-line trough from C IV). However, SMM 02399-0136 has a much stronger broad C III]1909 component and no splitting of the Lyα line. Also, the best estimates of the effects lensing for both objects make SMM 02399-0136 significantly more luminous than F10214+4724. Apart from possibly Si II there are no other low ionization UV features, and this, combined with the larger broad C III] component suggests that SMM 02399-0136 may be a little closer to 'face on' than is F10214+4724. The effects of differential magnification of the outer and inner NLRs in SMM 02399-0136 will be much less, because of the much smaller magnification gradient in the cluster lens, so that an infrared spectrum of this object should show more normal line ratios. The lack of a split in the Lyα line could be due to more isotropic radiation from the outer NLR contributing to the centre of the profile.

Hidden or patially hidden star formation in the obscuring tori of type-2 AGN may turn out to be common, and metal-rich outflows from these regions (for which we have evidence in F10214+4724) may stimulate starbursts in the remainder of the galaxy (Silk & Rees 1998). It is clear, though, from studies of F10214+4724 that disentangling the starburst, AGN and possibly lensing contributions to the observed infrared fluxes from similar objects discovered in future surveys will prove to be a major challenge. This may become possible, for example through very high-resolution imaging using interferometers working in the submm. If so, selection in the far-infrared/submm should prove to be much more reliable than UV flux for tracing the star formation history of the Universe.

ACKNOWLEDGMENTS

We are very grateful to Tom Geballe for obtaining the *J*-band spectrum as part of the UKIRT service programme, and to Chris Simpson for use of his software. We thank the referee, Neil Trentham, for a careful reading of the manuscript and for improving the discussion in Section 7. We also thank Michel Fioc and Brigitte Rocca-Volmerange for making their spectral synthesis models freely available. The UKIRT is operated by the Joint Astronomy Centre on behalf of the UK Particle Physics and Astronomy Research Council. This research has made use of the NASA/IPAC Extragalactic Database which is operated by the Jet Propulsion Laboratory, California Institute of Technology, under contract with the National Aeronautics and Space Administration.

REFERENCES

Antonucci R., Hurt T., Miller J.S., 1994, ApJ, 430, 210
Bohlin R.C., Savage B.D., Drake J.F., 1978, ApJ, 224, 132
Broadhurst T., Lehár J., 1995, ApJ, 450, L41
Bunker A.J., 1996, DPhil thesis, Univ. Oxford
Caganoff S. et al., 1991, ApJ, 377, L9
Calzetti D., Kinney A.L., Storchi-Bergmann T., 1994, ApJ, 429, 582
Cardelli J.A., Clayton G.C., Mathis J.S., 1989, ApJ, 345, 245
Condon J.J., 1992, ARA&A, 30, 575
Crenshaw D.M., 1997, in Peterson B.M., Cheng F.-Z., Wilson A.S., eds, ASP Conf. Proc. 113, Emission Lines in Active Galaxies: New Methods and Techniques. Astron. Soc. Pac., San Fransisco, p. 240
Davidson K., Netzer H., 1979, Rev. Mod. Phys., 51, 715
Dey A., van Breugel W., Vacca W.D., Antonucci R., 1997, ApJ, 490, 698
Downes D., Solomon P.M., Radford S.J.E., 1995, ApJ, 453, L65
Eales S.A., Rawlings S., 1993, ApJ, 411, 67
Eisenhardt P.R., Armus L., Hogg D.W., Soifer B.T., Neugebauer G., Werner M.W., 1996, ApJ, 461, 72
Elston R., McCarthy P.J., Eisenhardt P., Dickinson M., Spinrad H., Januzzi B.T., Maloney P., 1994, AJ, 107, 910
Ferguson J.W., Ferland G.J., Pradhan A.K., 1995, ApJ, 438, L55
Ferland G., Netzer H., 1979, ApJ, 229, 274
Fioc M., Rocca-Volmerange B., 1997, A&A, 326, 950
Gallego J., Zamorano J., Aragon-Salamanca A., Rego M., 1995, ApJ, 455, L1
George I.M., Turner T.J., Netzer H., Nandra K., Mushotzky R.F., Yaqoob T., 1998, ApJS, 114, 73
Goodrich R.W., Miller J.S., Martel A., Cohen M.H., Tran H.D., Ogle P.M., Vermeulen R.C., 1996, ApJ, 456, L9
Graham J.R., Liu M.C., 1995, ApJ, 449, L29
Green S.M., Rowan-Robinson M., 1996, MNRAS, 279, 884
Guiderdoni B., Bouchet F.R., Puget J.L., Lagache G., Hiron E., 1997, Nat, 390, 257
Heckman T., 1998, astro-ph/9801155, to appear in Proc. KNAW Colloq., The most distant radio galaxies
Heckman T.M., Gonzalez-Delgardo R., Leitherer C., Meurer G.R., Krolick J., Wilson A.S., Koratkar A., Kinney A., 1997, ApJ, 482, 114
Heisler C.A., Lumsden S.L., Bailey J.A., 1996, Nat, 385, 700
Hes R., Barthel P.D., Fosbury R.A.E., 1993, Nat, 362, 326
Ivison R., Smail I., Le Borgne J.F., Blain A.W., Knieb J.P., Bezecourt J., Kerr T.H., Davies J.K., 1998, MNRAS, in press
Iwamuro F., Maihara T., Tsukamoto H., Oya S., Hall D.B.N., Cowie L.L., 1995, PASJ, 47, 265
Kinney A.L., Bohlin R.C., Calzetti D., Panagia N., Wyse R.F.G., 1993, ApJS, 86, 5
Koski A.T., 1978, ApJ, 223, 56
Kriss G.A., Davidsen A.F., Blair W.P., Ferguson H.C., Long K.S., 1992, ApJ, 394, L37
Kroker H., Genzel R., Krabbe A., Tacconi-Garman L.E., Tecza M., Thatte N., Beckwith S.V.W., 1996, ApJ, 463, L55
Laor A., Draine B.T., 1993, ApJ, 402, 441
Lawrence A., Rigopoulou D., Rowan-Robinson M., McMahon R.G., Broadhurst T., Lonsdale C.J., 1994, MNRAS, 266, L41
Lowenthal J., Koo D., Guzman R., Gellego J., Phillips A., Faber S., Vogt N., Illingworth G., 1997, ApJ, 481, 673
Madau P., Pozzetti L., Dickinson M., 1998, ApJ, 498, 106
Mathews W.G., Veilleux S., 1989, ApJ, 336, 93
Matthews K. et al., 1994, ApJ, 420, L13 (M94)
Meurer G.R., Heckman T.M., Leitherer C., Kinney A., Robert C., Garnett D.R., 1995, AJ, 110, 2665
Netzer H., 1997, Ap&SS, 248, 127

Osterbrock D.E., 1989, Astrophysics of Gaseous Nebulae and Active Galactic Nuclei. University Science, Mill Valley CA
Osterbrock D.E., Fulbright J.P., 1996, PASP, 108, 183
Radford S.J.E., Downes D., Solomon P.M., Barrett J., Sage L.J., 1996, AJ, 111, 1021
Ramsay S.K., Mountain C.M., Geballe T.R., 1992, MNRAS, 259, 751
Rowan-Robinson, M. et al., 1991, Nat, 351, 719
Rowan-Robinson, M. et al., 1993, MNRAS, 261, 513
Rowan-Robinson M. et al., 1997, MNRAS, 289, 490
Salpeter E. E., 1955, ApJ, 121, 161
Scalo J. M., 1986, Fund. Cosmic Phys., 11, 1
Serjeant S., Lacy M., Rawlings S., King L.J., Clements D.L., 1995, MNRAS, 276, L31 (Paper I)
Serjeant S., Rawlings S., Lacy M., McMahon R., Lawrence A., Rowan-Robinson M., Mountain M., 1998, MNRAS, 298, 321 (Paper II)
Silk J., Rees M.J., 1998, A&A, 331, L1
Simpson C.J., Ward M.J., 1996, MNRAS, 282, 797
Smail I., Ivison R.J., Blain A.W., 1997, ApJ, 490, L5
Smith H.E., Lonsdale C.J., Lonsdale C.J., Diamond P.J., 1998, ApJ, 493, L17
Snijders M.H.J., Netzer H., Boksenberg A., 1986, MNRAS, 222, 549
Soifer B.T., Cohen J.G., Armus L., Matthews K., Neugebauer G., Oke J.B., 1995, ApJ, 443, L65
Trentham N., 1995, MNRAS, 277, 616
Verner D.A., Barthel P.D., Tytler D., 1994, A&AS, 108, 287

This paper has been typeset from a TEX/LATEX file prepared by the author.